Typhoon-Induced Strong Surface Flows in the Taiwan Strait and Pacific

YU-CHIA CHANG[1], RUO-SHAN TSENG[1]* and LUCA R. CENTURIONI[2]

[1]*Department of Marine Biotechnology and Resources, National Sun Yat-sen University, Kaohsiung 804, Taiwan,*
Also Kuroshio Research Group, Asia-Pacific Ocean Research Center, National Sun Yat-sen University, Kaohsiung 804, Taiwan
[2]*Scripps Institution of Oceanography, La Jolla, CA 92093-0213, U.S.A.*

(Received 3 January 2009; in revised form 2 October 2009; accepted 6 October 2009)

Surface Velocity Program drifters drogued at 15 m depth were deployed in the Taiwan Strait (TS) and Luzon Strait in 2005 and 2006. Several drifters in the TS and the Pacific were fortuitously overrun by the typhoon Hai-Tang (July 2005) and Shan-Shan (September 2006), respectively. The drifter and QuikSCAT wind data clearly demonstrate that the surface current over the TS and the Pacific can change dramatically for a period of about two days due to the strong winds of a typhoon during its passage. Our results show that the area of storm-affected surface currents is considerably smaller for a weaker typhoon (category 2 Shan-Shan), about 300~400 km in radius, than for a stronger typhoon (category 5 Hai-Tang), about 800 km in radius. The maximum observed current speed in the TS was 1.7 ms^{-1} (or 2.2 ms^{-1} in net speed change) under the influence of Hai-Tang, and 2 ms^{-1} in the Pacific under the influence of Shan-Shan. Drifter observations revealed the unusual phenomenon of flow reversal in the surface layer of TS and the Kuroshio induced by the typhoon passage. The effect of a typhoon on surface flows is amplified by the long, narrow geometry of the TS. Surface currents generated by wind forcing along the passage of a traveling typhoon can be explained by the Ekman drift.

Keywords:
· Surface Velocity Program drifter,
· typhoon,
· wind,
· surface current,
· Taiwan Strait,
· Ekman drift.

1. Introduction

One of the most devastating characteristics of a tropical cyclone (typhoon in the Pacific and hurricane in the Atlantic) is the strong wind along its passage. When a tropical cyclone passes over the sea surface, an enormous amount of momentum is injected into the ocean, resulting in strong mixing in the mixed layer and enhanced surface flows. Ocean observations, especially the mixed-layer currents, under a tropical cyclone are rare and difficult to make. To date, only a few reported observations of the upper ocean have been made beneath a hurricane. The upper ocean's response to three hurricanes has been examined using field observations and a numerical ocean model (Price *et al.*, 1994). From airborne expendable current profiler (AXCP) measurements, the maximum observed mixed-layer current varied from 0.8 ms^{-1} in response to hurricane Josephine, which was a large but comparatively weak hurricane, to 1.7 ms^{-1} in response to hurricane Gloria, which was very large and also intense (Price *et al.*, 1994). Zheng *et al.* (2006) analyzed the dataset of currents collected by two long-term NOAA moored buoys in the Gulf of Mexico, which were fortuitously overrun by a hurricane. They found that the shelf-break ocean responds almost immediately to the passage of a hurricane, and the oscillation peak-to-peak amplitudes in the surface layers strengthen to the order of 1 ms^{-1}. Oey *et al.* (2007) used satellite altimeter data to detect and verify forecast isopycnal motions under hurricanes in the Caribbean Sea and the Gulf of Mexico. Their work indicates that the presence of powerful ocean currents and coastal boundaries gives rise to intertwined hurricane-ocean interactions that in turn can modify the storm. Currents in excess of 2 ms^{-1} under Hurricane Ivan were observed on the shelf and slope in the northeastern Gulf of Mexico by an array of 14 acoustic Doppler current profilers (Teague *et al.*, 2007). Currents observed during the forced stage response were stronger to the left of the track on the shelf due to topographic constraints and more energetic to the

* Corresponding author. E-mail: rstseng@mail.nsysu.edu.tw

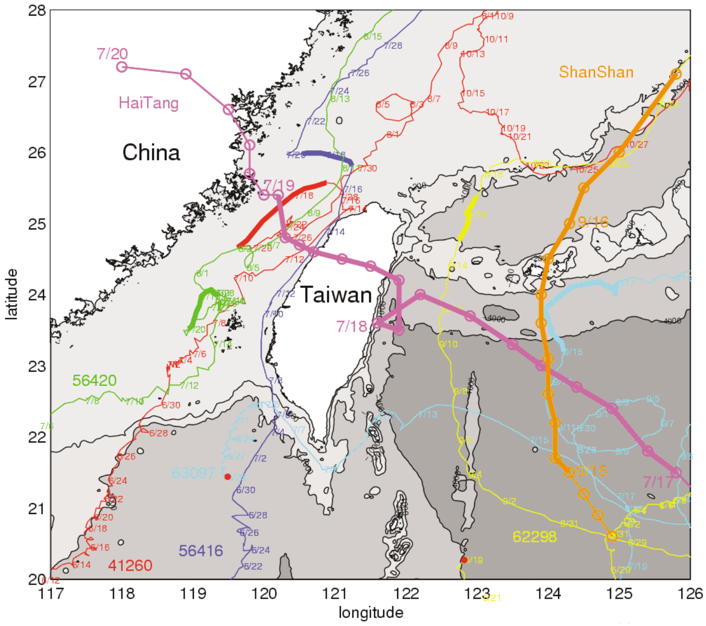

Fig. 1. Tracks of three drifters (41260, 56416 and 56420) in the TS and the associated Typhoon Hai-Tang (in magenta) in July 2005. Also shown are the tracks of two drifters (63097 and 62298) in the Pacific east of Taiwan and the associated Typhoon Shan-Shan (in orange) in September 2006. The duration during which drifters were affected by the typhoon are highlighted in bold.

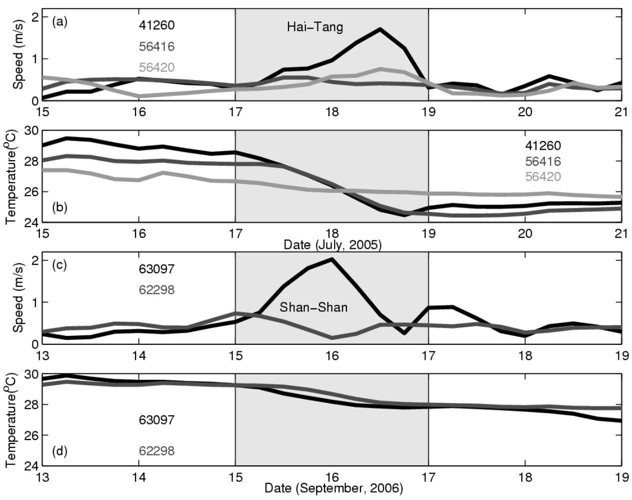

Fig. 2. (a) Total speed and (b) temperature observed by drifters 41260, 56416 and 56420 during Hai-Tang's passage in July 2005. (c) and (d) are as in (a) and (b) but for drifters 63097 and 62298 during Shan-Shan's passage in September 2006. Shadings denote the duration during which drifters were affected by the typhoon.

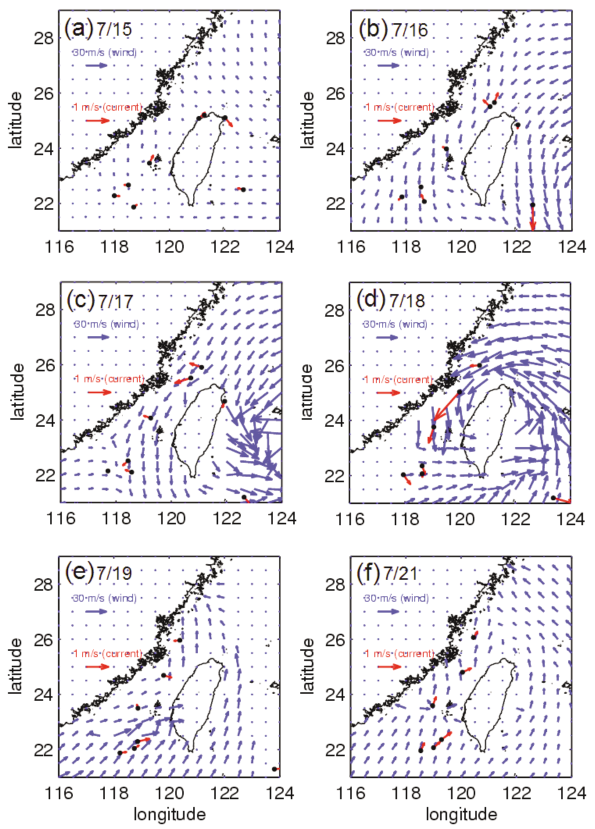

Fig. 3. Wind field (blue arrows) from QuikSCAT overlaid with drifter velocities (red arrows) at the date of (a) 15, (b) 16, (c) 17, (d) 18, (e) 19, and (f) 21 of July 2005.

right of the track, as expected, on the slope.

Taiwan Strait (TS) is a narrow channel separating China and Taiwan. The average width of the TS is about 160 km and the depth is mostly less than 60 m. Subtidal currents of the TS are controlled predominantly by the monsoonal wind condition and the pressure gradient. (Jan *et al.*, 2002). Connected with the northern TS is the East China Sea and its southeastern continental shelf with depth less than 300 m. Extending from northeastern Taiwan to Japan are the Ryukyu Islands, which separate the deeper Okinawa trough to the north and the Ryukyu trough to the south (Fig. 1). Each year several typhoons come from the Pacific, moving toward the west, which directly hit the Ryukyu Islands, Taiwan and the adjacent seas, causing huge losses of human life and property. A better understanding of the typhoon-induced currents in this region is important to the oceanographic communities in various respects, such as contaminant dispersal, material transport, and safety of navigation and offshore structure. In this study we use chance-encountered satellite-tracked drifter data to study the flow field of the TS and the Pacific east of Taiwan under the influence of Typhoon Hai-Tang and Shan-Shan during 2005 and 2006, respectively.

2. Data and Method

Information on Typhoon Hai-Tang (2005) and Shan-Shan (2006) was obtained from the best-track data from the Joint Typhoon Warning Center (http://metocph.nmci.navy.mil/jtwc.php). Synoptic wind fields over the TS and the adjacent seas were obtained from the NASA QuikSCAT ocean surface wind vectors. Wind retrievals of QuikSCAT were done on a 25 km × 25 km spatial scale and twice daily temporal coverage over a given geographic region. Direct velocity measurements in the surface mixed layer were obtained with Argos, satellite-tracked, Surface Velocity Program (SVP, Niiler, 2001) drifters drogued at a nominal depth of 15 m. Between October 2003 and December 2005, 259 SVP drifters were deployed by us in the Luzon Strait using volunteer observing ships to study the intrusion of Kuroshio into the South China Sea. Among these drifters, about ten of them, scattered in the TS and Pacific, were incidentally swept by Typhoon Hai-Tang during its passage in the summer of 2005. On the other hand, 12 drifters were deployed in the southern TS during June and July, 2006 to study the surface circulation of the TS and the adjacent seas. Most drifters moved eastward through the Luzon Strait to the region off the southeastern coast of Taiwan, and then either followed the Kuroshio to the north or continued to move further east to the Pacific. Among these drifters, about ten of them were also fortuitously overrun by Typhoon Shan-Shan along its track over the Pacific to the east of Taiwan in September, 2006. The 6-hourly positions and velocity drifter data were acquired online at http://www.aoml.noaa.gov/phod/dac/dacdata.html, the web site of NOAA/AOML.

3. Typhoon-Induced Strong Current in the TS and Pacific

Hai-Tang formed on July 11, 2005 at the Western subtropical Pacific as a poorly organized depression. As it moved westward it continued to gain strength, strengthening into a category-5 super-typhoon on July 16. On July 17 it weakened to category 3 as it continued west and made landfall at the eastern coast of Taiwan on the morning of July 18. It took a full day to cross the island of Taiwan, weakened to a minimal typhoon, and then entered the TS. On July 19 Hai-Tang made landfall for the second time near the southeastern China coast.

Shan-Shan was formed on September 9, 2006 at the western region of Guam as a tropical depression. It first moved toward the northwest, and then shifted to the westward direction along the 20°N and became a tropical storm and a typhoon on September 12. It then took a more north-northwesterly track on September 14, strengthened into a category-4 typhoon before passing Iriomote, Okinawa Islands, on September 15. Shan-Shan made landfall on September 17 on the island of Kyushu.

Figure 1 shows the tracks of Hai-Tang and Shan-Shan and the trajectories of five drifters (56416, 41260, 56420, 63097, 62298) which were most significantly and directly affected by these two typhoons. Note that drifters 56416, 41260 and 56420 were all traveling to the north in the TS before Hai-Tang approached Taiwan and changed the prevailing southwest summer monsoon wind field. Starting from July 17, 2005, drifter 56416 began to move westward in the northern TS, and drifters 41260 and 56420 began to move southward in the central and southern TS, respectively. The velocity magnitude and sea surface temperature observed by these three drifters are plotted in Figs. 2(a) and (b), demonstrating a significant enhancement of mixed-layer current and decrease of sea surface temperature induced by the typhoon. A maximum mixed-layer current speed of 1.7 ms^{-1} and temperature jump of about 4°C were observed by drifter 41260 in the central TS when this drifter was closest to the track of Hai-Tang. Chang *et al.* (2008) used the data of multi-satellite observation to demonstrate the occurrence of upwelling after the passage of Hai-Tang in the southern ECS. They also indicated that the SST fell rapidly to 24.2°C, a drop of 4.5°C. On the other hand, drifter 63097 initially moved slowly northward along approximately 124°E prior to the arrival of Shan-Shan during September 2006 (Fig. 1). Shan-Shan approached drifter 63097 on September 15 and the drifter speed increased dramatically to about 2 ms^{-1} (Fig. 2(c)), while the flow direction shifted to the east along the shelf (Fig. 1) and the SST showed a decrease of 2°C (Fig. 2(d)).

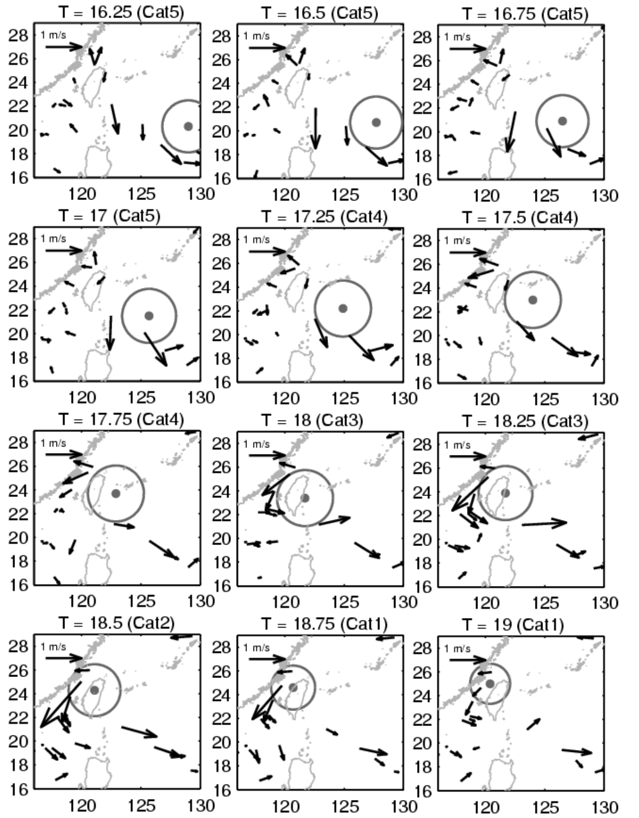

Fig. 4. Six-hourly distributions of surface currents and storm size during Hai-Tang's passage in July 2005. The storm radius is the radius for the 35-knot wind speed (circle). The storm intensity (in Saffir-Simpson Scale) and the indicated time (in month day) are also marked on the top of the plots.

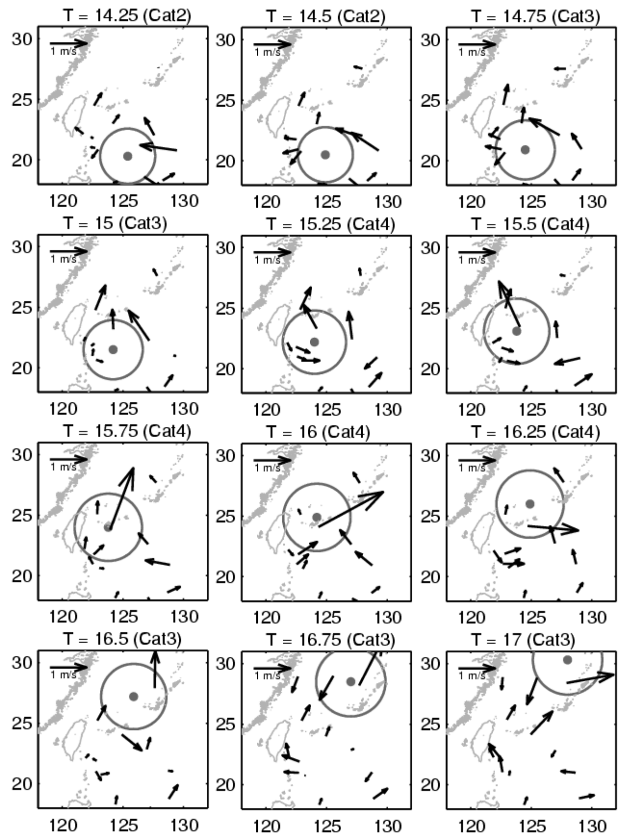

Fig. 5. As Fig. 4, but for Typhoon Shan-Shan during September 2006.

Figure 3 shows the daily distributions of the QuikSCAT wind and drifter speed in vectors during the period of 15–21 July 2005. A typical summer southwest monsoon pattern can be seen on July 15 (Fig. 3(a)), prior to the arrival of Hai-Tang with light winds of about 5 ms^{-1} over the TS and current speeds generally less than 0.3 ms^{-1}. On July 16 the wind condition in the TS was affected by Hai-Tang with a southwestward wind direction and the speed increased to 8~13 ms^{-1}. The mixed-layer currents in the TS, however, were still pointing to the north (Fig. 3(b)). Hai-Tang had its greatest impact on the wind and wave conditions of the TS during the next two days, July 17 and 18. The wind speeds enhanced to 17~23 ms^{-1} and the mixed-layer current speeds increased to about 0.8 ms^{-1} on July 17, both to the south (Fig. 3(c)). Maximum southwestward winds of 33 ms^{-1} and mixed-layer currents of 1.7 ms^{-1} were observed to occur in the northern TS in July 18 when Hai-Tang was centered in Taiwan (Fig. 3(d)). On July 19 Hai-Tang made landfall for the second time near the southeastern China coast, and a strong southwesterly wind was present in the TS, which brought heavy rainfall to the Southern Taiwan (Fig. 3(e)). The wind and current conditions were restored to the normal summer monsoon pattern on July 21 as Hai-Tang departed (Fig. 3(f)). This scenario demonstrates that the wind and current field over the TS changed rapidly and dramatically during a time span of about two days when a typhoon passed through Taiwan.

Previous studies have indicated that the current in the TS persists northeastward in all seasons but is strongly wind-dependent (Beardsley *et al*., 1985; Chuang, 1986; Fang *et al*., 1991; Zhu *et al*., 2004; Yang, 2007). The current profiles and volume transport observed in the TS during October and November 1999 from four bottom-mounted ADCPs showed strong reversals during strong northeast monsoon events (Lin *et al*., 2005), which might be explained by a combination of local wind effects and coastally trapped waves remotely generated in the Yellow Sea and ECS by the wintertime wind bursts (Ko *et al*., 2003). The present study indicates that besides the strong northeast monsoon events, typhoon is another important factor that generates current reversal in the TS.

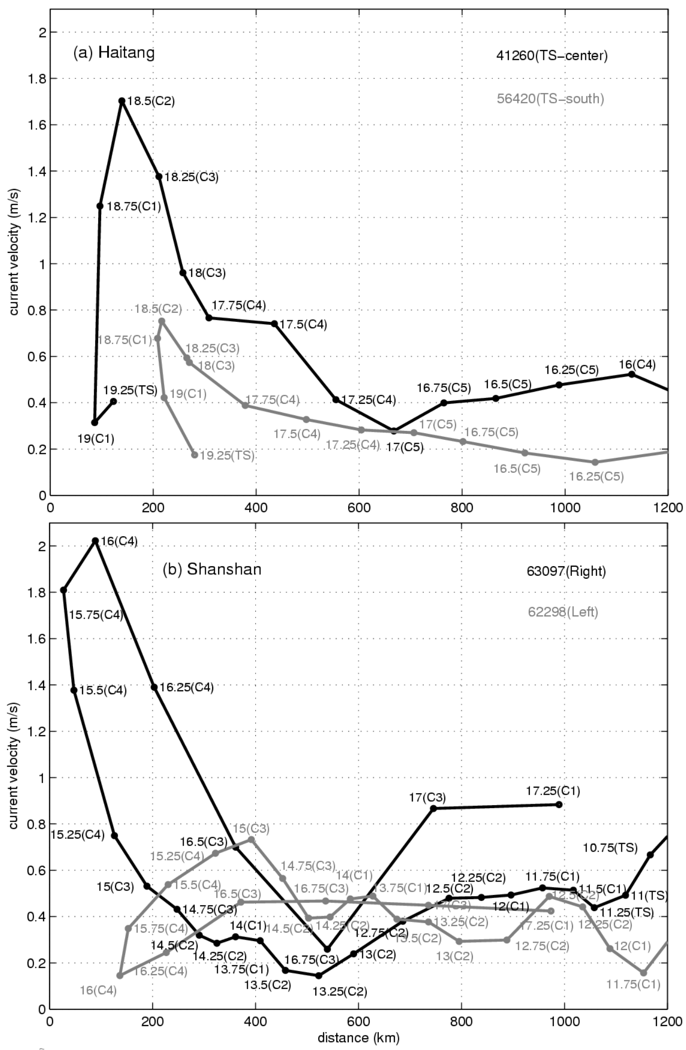

Fig. 6. Current speed of drifters under the influence of (a) Hai-Tang and (b) Shan-Shan in chronological order versus the distance from drifter to storm center. Storm intensity (Saffir-Simpson Scale) and indicated time (in month day) are also marked.

As typhoons with sufficient intensity pass through the TS, strong southward flows in the TS will appear and last for about two days.

4. Relationship between Surface Current, Typhoon and Channel Geometry

Figures 4 and 5 are plots of the distributions of surface currents derived from 6-hourly drifter data overlaid with the concurrent storm position, shown as a circle for typhoons Hai-Tang and Shan-Shan, respectively. In these two figures the storm radius is the radius of the 35-knot wind speed and the storm intensity is marked by the corresponding Saffir-Simpson hurricane scale (category 1~5). In order to demonstrate the typhoon-induced surface currents against the distance from the storm center, current speeds derived from drifters 41260 and 56420 are plotted in Fig. 6(a), in chronological order against the distance between the drifters and the center of Hai-Tang. A similar plot is shown in Fig. 6(b) for the case of typhoon Shan-Shan and drifters 63097 and 62298. Tables 1 and 2 also list the 6-hourly typhoon intensity, distance between the typhoon center and drifter, and the corresponding drifter speed and direction for Hai-Tang and Shan-Shan, respectively. The QuikSCAT wind speeds and directions interpolated onto the position of the drifters are also included in these two tables. At 06:00 UTC 16 July 2005, when Hai-Tang was in category 5 and about 980 km east of TS, drifters observed northward flows in the TS with a speed of about 0.5 ms^{-1}. This was the prevailing flow pattern in the TS during summertime, which implies that at this distance the influence of Hai-Tang on surface currents of the TS was not yet felt. However, the

Table 1. Information on Typhoon Hai-Tang and drifter 41260. QuikSCAT winds were interpolated into the drifter position to obtain wind speed and direction. Numbers in parentheses indicate the QuikSCAT data retrieval time expressed in day of month. Both wind and current are expressed as flows towards a given direction.

Time (UTC)	Typhoon scale (Saffir-Simpson)	Distance (km)	Wind speed (ms^{-1})	Wind direction	Current speed (ms^{-1})	Current direction
06:00 16 July	category 5	980	12 (t = 16.37)	SW	0.5	NNW
12:00 16 July	category 5	860	*	*	0.4	NW
18:00 16 July	category 5	770	*	*	0.4	WNW
00:00 17 July	category 5	670	13 (t = 16.90)	SSW	0.3	W
06:00 17 July	category 4	560	19 (t = 17.36)	SSW	0.4	WSW
12:00 17 July	category 4	430	*	*	0.7	WSW
18:00 17 July	category 4	310	*	*	0.8	WSW
00:00 18 July	category 3	260	27 (t = 17.88)	S	1.0	SW
06:00 18 July	category 3	210	*	*	1.4	SW
12:00 18 July	category 2	130	33 (t = 18.41)	S	1.7	SW
18:00 18 July	category 1	100	*	*	1.2	SW
00:00 19 July	category 1	80	8 (t = 19.92)	NE	0.3	SW

Table 2. As Table 1, but for Typhoon Shan-Shan and drifter 63097.

Time (UTC)	Typhoon scale (Saffir-Simpson)	Distance (km)	Wind speed (ms^{-1})	Wind direction	Current speed (ms^{-1})	Current direction
12:00 12 Sep.	category 2	780	4 (t = 12.40)	NW	0.5	NNE
18:00 12 Sep.	category 2	680	*	*	0.4	NE
00:00 13 Sep.	category 2	590	*	*	0.2	NNE
06:00 13 Sep.	category 2	520	*	*	0.1	NNE
12:00 13 Sep.	category 2	450	*	*	0.2	N
18:00 13 Sep.	category 1	410	13 (t = 13.85)	S	0.3	N
00:00 14 Sep.	category 1	360	*	*	0.3	NNE
06:00 14 Sep.	category 2	320	*	*	0.3	NNE
12:00 14 Sep.	category 2	290	14 (t = 14.43)	W	0.3	N
18:00 14 Sep.	category 3	250	*	*	0.4	N
00:00 15 Sep.	category 3	180	18 (t = 14.90)	W	0.5	N
06:00 15 Sep.	category 4	120	*	*	0.5	NNW
12:00 15 Sep.	category 4	40	33 (t = 15.41)	NW	1.4	NNW
18:00 15 Sep.	category 4	20	*	*	1.8	NNE
00:00 16 Sep.	category 4	80	32 (t = 15.88)	NNE	2.0	NE
06:00 16 Sep.	category 4	200	*	*	1.4	E
12:00 16 Sep.	category 3	370	16 (t = 16.40)	E	0.7	SEE
18:00 16 Sep.	category 3	540	*	*	0.3	NNE

flows off the eastern coast of Taiwan were greatly affected by Hai-Tang at T = 16.25, as can be seen from the southward flowing Kuroshio (Fig. 4). Note that the wind direction in the TS as Hai-Tang approached was opposite to the prevailing flow direction. Six hours later, at 12:00 UTC 16 July as Hai-Tang was located at 860 km east of TS, the current speed in the TS started to decrease and the flow direction gradually shifted westward (Table 1). The flow speed decrease and veering direction continued as Hai-Tang approached Taiwan and its intensity weakened. A strongest typhoon-induced surface current in the TS, with a speed of 1.7 ms^{-1} and a southwestward direction, was observed at approximately 130 km to the west of Hai-Tang; the corresponding wind speed at the drifter position was 33 ms^{-1}, blowing toward the south. A close examination of the current and wind directions in the TS under the influence of the typhoon (Table 1) indicates that the currents generally flow to the right of the wind direction with a deviation angle of roughly 45° or less, which is consistent with the Ekman theory. Since the orientation of the TS is nearly NE-SW, the most favorable wind direction for the Ekman drift is southward. It is interesting to note that when Hai-Tang's center was located at the TS and was closest to drifter 63097 (80 km distance) at July 19, the surface current was not very strong, being only 0.3 m/s toward the SW. The cause of this seemingly contradictory finding is that at this closest distance the typhoon-induced wind direction veered further toward the east and was thus unfavorable for the generation of Ekman drift in the TS.

Drifter 56420 was in the southern TS when Hai-Tang attacked. A maximum typhoon-induced surface current speed of 0.78 ms^{-1} toward the SW was observed by this drifter at a distance of approximately 220 km to the west of Hai-Tang. Note that the typhoon-induced surface current at the southern TS observed by drifter 56420 was substantially slower than that at the northern TS observed by drifter 41260, while both drifters were at about the same distance from Hai-Tang (Fig. 6(a)). This difference can be attributed to their relative positions with respect to the typhoon and the channel orientation of TS. The effect of a typhoon on surface flows is amplified considerably by the long, narrow geometry of the northern TS and when the typhoon-induced wind direction is more favorable to the generation of Ekman drift in the TS.

The case of Shan-Shan differs from that of Hai-Tang in several respects. Shan-Shan was a category-2 typhoon in the early stage, later intensifying to category 4 with a nearly northward track at about 200 km east of Taiwan. The region over which drifters 63097 and 63398 drifted was overrun by Shan-Shan near the south end of the Ryukyu islands with depths over 1000 m. Flow directions of the surface mixed-layer currents near or within the storm radius generally have a tendency to diverge around the typhoon, and the current speed increased as the distance from the storm center decreased (Fig. 5). Outside the storm radius the surface mixed-layer currents did not seem to be greatly affected by Shan-Shan, as can be seen from the northward-flowing Kuroshio off the northeastern coast of Taiwan on September 14 (Fig. 5). Thus the area of storm-affected surface currents is considerably smaller for a weaker typhoon (category 2), about 300~400 km in radius, than for a stronger typhoon (category 5), about 800 km in radius, as is the case for Hai-Tang. Drifter 63097 was moving to the north at a speed of about 0.5 ms^{-1} prior to the influence of Shan-Shan (Table 2). As Shan-Shan approached from the south, the northward speed of drifter 63097 lessened slightly due to the opposition of the wind and current directions. From September 15.25, Shan-Shan intensified to category 4 and several drifters (including 63097) were caught within the storm radius and all moved consistently in a cyclonic direction. From September 15.5 to 16, drifter 63097 was to the right of the track of Shan-Shan with a close separation of about 20~80 km from the center; the observed current speeds reached a maximum value of 1.4~2.0 ms^{-1}, while the wind speed at the drifter position was about 33 ms^{-1} (Table 2). These represent rare, valuable Lagrangian observations of surface currents very close to a typhoon's center. The surface currents affected by Shan-Shan in the Pacific also flow to the right of the wind direction (Table 2). Therefore, the surface currents generated by wind forcing under the influence of typhoons in the TS and the Pacific can be explained quite nicely by classical Ekman drift theory. However, whether the Ekman drift current is fully developed by the traveling typhoon still needs further study.

Drifter 62298, which was located off the northeastern coast of Taiwan and moved northward along the edge of the Kuroshio with a speed of about 0.8 ms^{-1} on September 15 (Fig. 5), was first outside the storm radius and was not affected by Shan-Shan. During September 15.5 to 16.0, when this drifter was within the storm radius and to the left of the track, the northward-flowing Kuroshio can be seen to slow down significantly (from 0.8 ms^{-1} to 0.1 ms^{-1}, Fig. 2), almost becoming stagnant. Afterwards, it quickly resumed its original state, flowing north. Numerical simulations of Tsai *et al.* (2008) also indicate that the northward-flowing Kuroshio and the complicated flow field off northeastern Taiwan could be dramatically altered by the passage of typhoons. The Lagrangian observations presented in this paper under the influence of a category-4 typhoon agree with the modeled results.

5. Conclusion

This study provides direct, valuable evidence of the enhanced surface flows induced by a typhoon's passage in the TS and the Pacific during July 2005 and September 2006. Our results indicate that the typhoon-induced strong flows and current reversal only last for a typical period of about two days. Surface currents within the radius of about 860 km from a category-5 typhoon center are strongly affected by the winds and the flows tend to be divergent around the typhoon. Surface current speeds increase as the distance from the storm center decreases, and current directions flow to the right of the wind directions. Therefore, surface currents generated by wind forcing along the typhoon passage can be explained by Ekman drift. The maximum observed surface current speed was 2 ms^{-1} at 100 km away from the center of a category-4 typhoon Shan-Shan in the Pacific, and was 1.7 ms^{-1} southward at 120 km from the center of a category-2 typhoon Hai-Tang in the TS. Note that the pre-typhoon surface flow in the TS was the prevailing summer monsoonal flow pattern, i.e., around 0.5 ms^{-1} toward the north. Therefore, typhoon Hai-Tang produced a net southward current of 2.2 ms^{-1} in the TS, which implies that the typhoon-induced current is stronger in a channel than in the Pacific or an open ocean. The swift Kuroshio near the surface could be slowed down or even reversed by the typhoon, depending on the intensity of and separation from the typhoon. The area of storm-affected surface currents is considerably smaller for a weaker typhoon (category 2), about 300~400 km in radius, than for a stronger typhoon (category 5), about 800 km in radius as for the case of Hai-Tang.

Acknowledgements

This work was supported by the National Science Council of the Republic of China under contract NSC95-2611-M-110-009-MY3. We are grateful for the comments of two anonymous reviewers.

References

Beardsley, R. C., R. Limeburner and H. Yu (1985): Discharging of the Changjiang (Yangtze River) into the East China Sea. *Cont. Shelf Res.*, **4**, 57–76.

Chang, Y., H.-T. Liao, M.-A. Lee, J.-W. Chan, W.-J. Shieh, K.-T. Lee, G.-H. Wang and Y.-C. Lan (2008): Multisatellite observation on upwelling after the passage of Typhoon Hai-Tang in the southern East China Sea. *Geophys. Res. Lett.*, **35**, L03612, doi:10.1029/2007GL032858.

Chuang, W.-S. (1986): A note on the driving mechanism of current in the Taiwan Strait. *J. Oceanogr. Soc. Japan*, **42**, 355–361.

Fang, G., B. Zhao and Y. Zhu (1991): Water volume transport through the Taiwan Strait and the continental shelf of the East China Sea measured with current meters. p. 345–358. In *Oceanography of Asian Marginal Seas*, ed. by K. Takano, Elsevier.

Jan, S., J. Wang, C.-S. Chern and S.-Y. Chao (2002): Seasonal variation of the circulation in the Taiwan Strait. *J. Mar. Sys.*, **35**. 249–268.

Ko, D. S., R. H. Preller, G. A. Jacobs, T. Y. Tang and S. F. Lin (2003): Transport reversals at Taiwan Strait during October and November 1999. *J. Geophys. Res.*, **108**(C11), 3370, doi:10.1029/2003JC001836.

Lin, S. F., T. Y. Tang, S. Jan and C.-J. Chen (2005): Taiwan strait current in winter. *Cont. Shelf Res.*, **25**, 1023–1042.

Niiler, P. P. (2001): The world ocean surface circulation. p. 193–204. In *Ocean Circulation and Climate*, ed. by G. Siedler *et al.*, Academic Press.

Oey, L. Y., T. Ezer, D.-P. Wang, X.-Q. Yin and S.-J. Fan (2007): Hurricane-induced motions and interaction with ocean currents. *Cont. Shelf Res.*, **27**, 1249–1263.

Price, J. F., T. B. Sanford and G. Z. Forristall (1994): Forced stage response to a moving hurricane. *J. Phys. Oceanogr.*, **24**, 233–260.

Teague, W. J., E. Jarosz, D. W. Wang and D. A. Mitchell (2007): Observed oceanic response over the upper continental slope and outer shelf during hurricane Ivan. *J. Phys. Oceanogr.*, **37**, 2181–2206.

Tsai, Y., C.-S. Chern and J. Wang (2008): Typhoon induced upper ocean cooling off northeastern Taiwan. *Geophys. Res. Lett.*, **35**, L14605, doi:10.1029/2008GL034368.

Yang, J. (2007): An oceanic current against the wind: How does Taiwan Island steer warm water into the East China Sea? *J. Phys. Oceanogr.*, **37**, 2563–2569.

Zheng, Q., R. J. Lai, N. E. Huang, J. Pan and W. T. Liu (2006): Observation of ocean current response to 1998 Hurricane Georges in the Gulf of Mexico. *Acta Oceanol. Sinica*, **25**, 1–15.

Zhu, J., C. Chen, P. Ding, C. Li and H. Lin (2004): Does the Taiwan warm current exist in winter? *Geophys. Res. Lett.*, **31**, L12302, doi:10.1029/2004GL019997.